PRIMARY RESEARCH ARTICLE

Global Change Biology WILEY

Increasing picocyanobacteria success in shelf waters contributes to long-term food web degradation

Katrin Schmidt[1] | Antony J. Birchill[1] | Angus Atkinson[2] | Robert J. W. Brewin[2,3] | James R. Clark[2] | Anna E. Hickman[4] | David G. Johns[5] | Maeve C. Lohan[4] | Angela Milne[1] | Silvia Pardo[2] | Luca Polimene[2] | Tim J. Smyth[2] | Glen A. Tarran[2] | Claire E. Widdicombe[2] | E. Malcolm S. Woodward[2] | Simon J. Ussher[1]

[1]School of Geography, Earth and Environmental Sciences, University of Plymouth, Plymouth, UK

[2]Plymouth Marine Laboratory, Plymouth, UK

[3]College of Life and Environmental Sciences, University of Exeter, Penryn, UK

[4]Ocean and Earth Sciences, University of Southampton, National Oceanography Centre, Southampton, UK

[5]Marine Biological Association, Plymouth, UK

Correspondence
Katrin Schmidt, School of Geography, Earth and Environmental Sciences, University of Plymouth, Plymouth, UK.
Email: katrin.schmidt@plymouth.ac.uk

Abstract

Continental margins are disproportionally important for global primary production, fisheries and CO_2 uptake. However, across the Northeast Atlantic shelves, there has been an ongoing summertime decline of key biota—large diatoms, dinoflagellates and copepods—that traditionally fuel higher tropic levels such as fish, sea birds and marine mammals. Here, we combine multiple time series with in situ process studies to link these declines to summer nutrient stress and increasing proportions of pico-phytoplankton that can comprise up to 90% of the combined pico- and nanophytoplankton biomass in coastal areas. Among the pico-fraction, it is the cyanobacterium *Synechococcus* that flourishes when iron and nitrogen resupply to surface waters are diminished. Our field data show how traits beyond small size give *Synechococcus* a competitive edge over pico- and nanoeukaryotes. Key is their ability to grow at low irradiances near the nutricline, which is aided by their superior light-harvesting system and high affinity to iron. However, minute size and lack of essential biomolecules (e.g. omega-3 polyunsaturated fatty acids and sterols) render *Synechococcus* poor primary producers to sustain shelf sea food webs efficiently. The combination of earlier spring blooms and lower summer food quantity and quality creates an increasing period of suboptimal feeding conditions for zooplankton at a time of year when their metabolic demand is highest. We suggest that this nutrition-related mismatch has contributed to the widespread, ~50% decline in summer copepod abundance we observe over the last 60 years. With *Synechococcus* clades being prominent from the tropics to the Arctic and their abundances increasing worldwide, our study informs projections of future food web dynamics in coastal and shelf areas where droughts and stratification lead to increasing nutrient starvation of surface waters.

KEYWORDS
climate change, copepods, food quality, iron, nitrate, picoeukaryotes, stratification, *Synechococcus*, time series, Western Channel Observatory

1 | INTRODUCTION

The global importance of continental margins arises from sustained nutrient supply via river discharge, dust deposition and exchange with shallow sediments. The high nutrient availability favours the 'classical pelagic food chain' with large primary producers, intensive phytoplankton blooms, abundant mesozooplankton (e.g. copepods) and efficient carbon transfer to higher trophic levels such as fish, seabirds and marine mammals (Kiørboe, 2008). About 80% of the world's wild-captured seafood derives from coastal and shelf seas (Watson, Green, Tracey, Farmery, & Pitcher, 2016) and marine lipids and proteins are in high demand for uses in human consumption, aquaculture, agriculture and health (Chassot et al., 2010; Greenberg, 2018).

However, there are indications that with climate change, the productivity of shelf areas is declining. The well-studied North Sea (Northeast Atlantic) represents a prime example. Here, reductions in euphausiid and copepod abundance and copepod size have been recorded since the 1980s, with negative implications for fish stock recruitment (Beaugrand, Brander, Lindley, Souissi, & Reid, 2003; Capuzzo et al., 2017).

Two mechanisms have been proposed for these changes in zooplankton abundance. On the one hand are direct effects of rising temperature (Beaugrand, Reid, Ibanez, Lindley, & Edwards, 2002) and on the other hand are indirect effects of warming and de-eutrophication that act via the overall food availability (Capuzzo et al., 2017). As a direct response to rising temperatures, many terrestrial and marine species shift their biogeographical range towards the poles (Parmesan & Yohe, 2003). North Atlantic warm-water copepod species have moved polewards by up to 260 km per decade between 1958 and 1999, and replaced cool-water copepods in the North Sea (Beaugrand et al., 2002). As the warm-water copepod assemblages have typically lower biomass and contain smaller species, changes in the food web of the North Sea have been linked to these shifts in species distribution (Beaugrand et al., 2003).

In addition to direct physiological effects, rising temperatures can also have indirect effects on food web relationships. Larger heat absorption of the ocean strengthens surface stratification, which hinders nutrient exchange with deeper water and can lead to nutrient limitation of phytoplankton and decreasing net primary production (Bopp et al., 2013). For the North Sea, such a decline in primary production over the last 25 years has been linked to reductions in zooplankton abundance and fish stock recruitment (Capuzzo et al., 2017). A co-occurring shift in the spring bloom phenology, with an earlier formation and termination of the bloom (Desmit et al., 2020; Friedland et al., 2018), is in line with an earlier annual start of water column stratification due to climate change (Holt, Wakelin, Lowe, & Tinker, 2010).

However, nutrient limitation affects not only net primary production but also the phytoplankton community structure. A key prognosis of climate warming effects, the shift towards smaller primary producers, is backed up by geological records (Finkel et al., 2007), modelling approaches (Dutkiewicz, Scott, & Follows, 2013), in situ monitoring (Agirbas et al., 2015) and satellite observations (Brewin et al., 2012). Advantages of decreased cell size are a thinning of the cell boundary layer and increase in nutrient diffusion per unit of cell volume (Raven, 1998), which rapidly decreases the nutrient concentration required for saturated growth rates (Chrisholm, 1992). Thus, growth of picophytoplankton is saturated at ambient nitrate concentrations of >0.2 μM, while maximum growth rates of diatoms require 0.7–1.0 μM nitrate (Agawin, Duarte, & Agustí, 2000). In stratified shelf seas of the North East Atlantic, nitrate concentrations <0.2 μM and iron concentrations <0.2 nM are not exceptional (Birchill et al., 2017, 2019), indicating that species' efficient nutrient uptake and/or storage will be key. However, picophytoplankton is too small to be grazed by copepods (Kiørboe, 2008) and non-diatom phyla often lack essential biomolecules such as omega-3 polyunsaturated fatty acids and sterols (Jónasdóttir, 2019; Ruess & Müller-Navarra, 2019). Therefore, the efficiency and quality of shelf sea food webs in a warming climate will depend on direct temperature effects (Beaugrand et al., 2003), on total primary production (Capuzzo et al., 2017) and also on the size and taxonomic composition of the dominant primary producers (Schmidt, Kähler, & von Bodungen, 1998).

To understand how climate change may impact the community structure at the base of the food web in shelf seas, we approached the problem at two scales. Large temporal and spatial resolution, as provided by satellite earth observations and the Continuous Plankton Recorder (CPR) survey, allowed us to identify (a) differences between longer term (60 years) and shorter term (20 year) changes, (b) the spatial extent of changes and (c) the months that are most affected. At the smaller scale, we use intensive field observations of the phytoplankton community along a coast–shelf–shelf break gradient of nutrient supply as a 'natural experiment' to reveal the mechanisms that drive the success of the various primary producers. By linking the two scales, we provide a conceptual model of why the classical food web is increasingly under threat in temperate coastal and shelf areas.

2 | MATERIALS AND METHODS

2.1 | Continuous Plankton Recorder survey

The CPR survey has operated in the North Atlantic since 1931 and is currently managed by the Marine Biological Association (Plymouth). The collection and analysis of CPR samples have followed a consistent methodological approach since 1958, with details given in Richardson et al. (2006). In brief, the CPR collects samples using a high-speed plankton recorder that is towed behind 'ships of opportunity' through the surface layer of the ocean (~10 m depth). Water passes through the recorder, and plankton are filtered by a slow moving silk layer (mesh size 270 μm). A second layer of silk covers the first and both are reeled into a tank containing 4% formaldehyde, and thereby preserved for later analysis.

We collated a 60 year time series (1958–2017) from 16 CPR subareas in the NE Atlantic, covering an area of ~2,000 × 1,500 km

(Figure 1a) and based on 136,903 samples. Our data set comprises only species/genera that have continuously been identified since 1958, including 65 diatoms, 53 dinoflagellates and the seven most abundant copepods. In the case of the *Calanus* spp., we distinguished between early *Calanus* copepodites (CI-IV; no species level) and late copepodites (CV/adults of *Calanus finmarchicus* and *Calanus*

helgolandicus). The smaller copepods were only identified to genus level (*Oithona* spp., *Acartia* spp., *Paracalanus* spp., *Pseudocalanus* spp.) or the species were merged for analysis (*Centropages hamatus* and *Centropages typicus*), with the exception of *Temora longicornis*. DOIs of the individual data sets are provided in the References section (Johns, 2019).
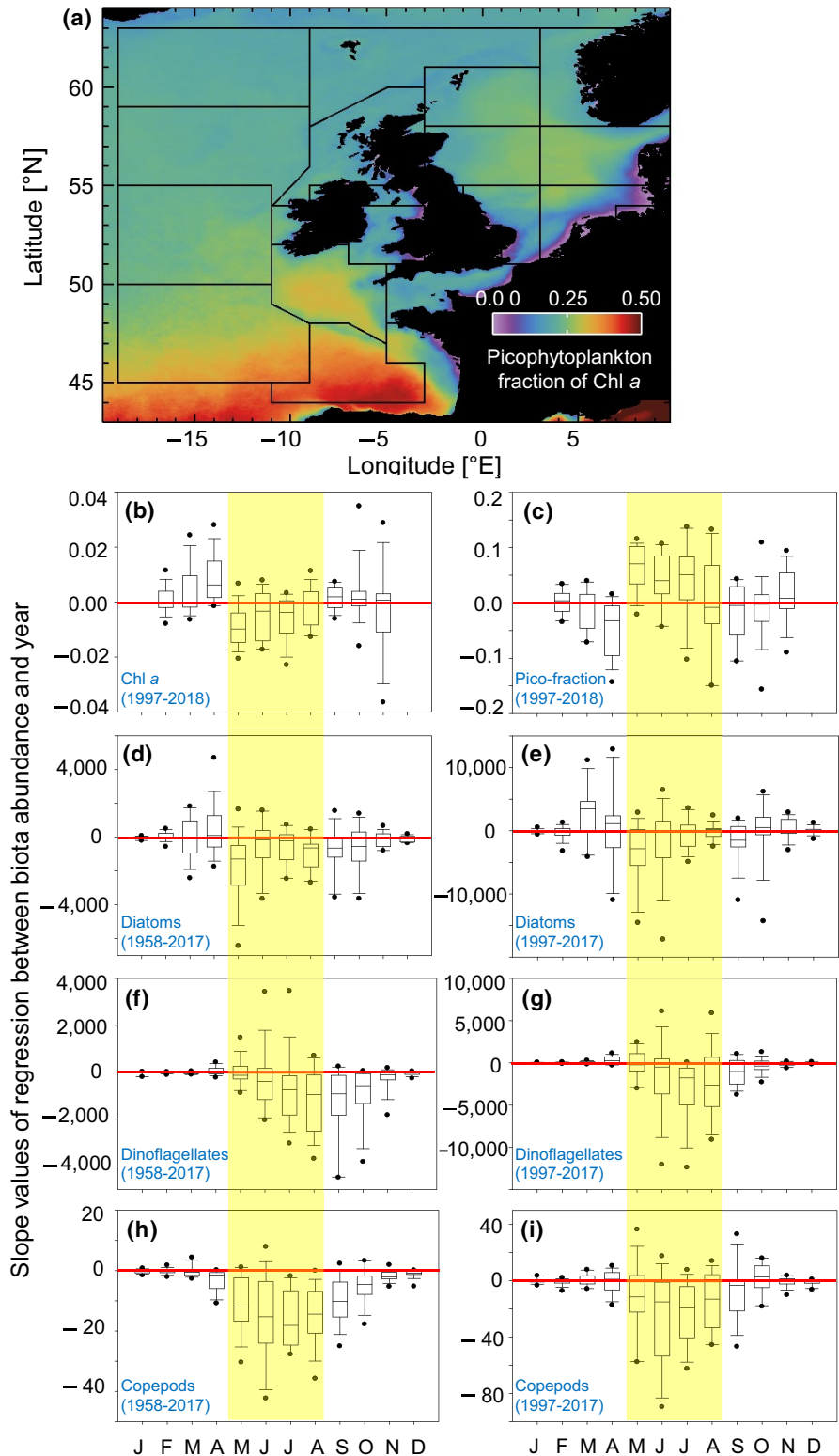
FIGURE 1 Summer reductions in Chl *a*, diatoms, dinoflagellates and copepods, but an increasing picophytoplankton fraction across temperate shelf areas of the NE Atlantic. Results from Continuous Plankton Recorder (CPR) data (1958–2017) and satellite-derived ocean colour data (1997–2018). (a) Picophytoplankton fraction of Chl *a* during summer (July), climatology 1998–2018. The grid shows the 16 subareas that were considered for our data analysis. (b–i) Slope values for the regression between monthly median abundance over the last 20 years (i.e. =satellite era) and over the last 60 years (i.e. =CPR era). The vertical boxes and error bars indicate the median, 10th, 25th, 75th and 90th percentiles of the data (*n* = 16). (b) Chl *a* concentrations, (c) picophytoplankton fraction of Chl *a*, (d) diatoms (1958–2017), (e) diatoms (1997–2017), (f) dinoflagellates (1958–2017), (g) dinoflagellates (1997–2017), (h) copepods (1958–2017), (i) copepods (1997–2017). The late spring to summer period, where most of the changes occur, is highlighted in yellow. For this period (May–August), nonparametric Wilcoxon signed rank tests showed that slope values were overall significantly different from zero. Wilcoxon statistics: Panel (b) 391 (*p* < .001); (c) 1,584 (*p* < .001); (d) 367 (*p* < .001); (e) right 542 (*p* = .019); (f) 438 (*p* < .001); (g) 377 (*p* < .001); (h) 30 (*p* < .001); (i) 224 (*p* < .001). *n* = 64

2.2 | Satellite data

Chlorophyll data were extracted for the same 16 subareas of the NE Atlantic as the CPR survey. The regional monthly chlorophyll climatology maps are calculated by averaging monthly chlorophyll values on a pixel-by-pixel basis over the 1997–2018 period. The monthly time series are computed by averaging monthly chlorophyll values over the different regions of interest. Both the time series and the climatology maps were calculated using the global merged multi-sensor product OCEANCOLOUR_GLO_CHL_L3_REP_OBSERVATIONS_009_065 distributed by the Copernicus Marine Environment Monitoring Service (CMEMS, 2018). This product was derived from the OC-CCI v4.0 data set produced by the ESA Ocean Colour Climate Change Initiative (ESA OC-CCI, Sathyendranath et al., 2018).

The picophytoplankton fractions were computed using the phytoplankton group satellite model of Brewin et al. (2017). The model estimates the fraction of total chlorophyll a by picophytoplankton using satellite estimates of total chlorophyll a and sea surface temperature (SST) as input (see Brewin et al., 2017 for further details on the algorithm). Daily total chlorophyll a satellite data, from version 4.0 of the Ocean Colour Climate Change Initiative (OC-CCI, geographic projection, processed using the OC3 chlorophyll a algorithm, data downloaded at http://www.oceancolour.org/) and SST, from the Optimal Interpolation Sea Surface Temperature (OISST) data set (Version 2.0; Reynolds et al., 2007) acquired from the NOAA website (https://www.esrl.noaa.gov/psd/data/gridded/data.noaa.oisst.v2.highres.html) re-gridded to the same resolution as the OC-CCI data, were used in this study as input to the Brewin et al. (2017) model, for the period 1997–2018. Monthly products were produced by binning and averaging the data at each grid point, and climatology maps were calculated by averaging monthly chlorophyll values on a pixel-by-pixel basis over the 1997–2018 period. The monthly time series are computed by averaging monthly chlorophyll values over the different regions of interest.

2.3 | Sampling at the coastal monitoring site in the English Channel

The coastal monitoring site L4 (50°15′N, 4°13′W) is situated in the Western English Channel, about 15 km southwest of Plymouth (UK) and has a water column depth of ~54 m (Figure 2a). Weekly sampling at this site was established in 1988, but here we only consider data since 2007 when analytical flow cytometry counts were included in the list of acquired parameters. Vertical profiles of temperature, salinity, depth and Chl a were measured using a CTD system (SeaBird 19+) equipped with a fluorescence sensor (Smyth et al., 2010). Seawater for nutrient assays was collected from Niskin bottles attached to the CTD/Rosette system, and taken into acid clean, 'aged', 60 ml HDPE (Nalgene) sample bottles. Sampling depths were at 2 m (2007–2011) or at 2, 10, 25 and 50 m (since 2012). Clean sample and handling techniques were used. Samples were kept cool and in the dark and returned to the laboratory for analysis as soon as possible after arrival. Samples for flow cytometry analysis were collected from 2, 10, 25 and

50 m depth using 10 L Niskin bottles, returned to the laboratory within 3 hr and processed immediately. Samples for the enumeration of phytoplankton (≥10 μm) were collected at 10 m depth. The Tamar River is the main source of freshwater inflow to the Western English Channel, with a range of 5–140 m³/s at its mouth. Daily mean flow data for the Tamar River at Gunnislake were kindly provided by the National River Flow Archive (2007–2017) and the UK Environment Agency (2018).

2.4 | Sampling in the Celtic Sea

Sampling of 20 stations across the inner shelf, outer shelf and shelf break took place during two cruises in 2015 (April, July) on board the R.R.S. *Discovery*. An overview of the stations and sampled parameters is given in Table S1. Vertical profiles of temperature, salinity, depth and Chl a were measured using a CTD system (SeaBird 9/11+). Seawater for macronutrient analyses was collected from Niskin bottles attached to the CTD/Rosette system, and taken into acid clean, 'aged', 60 ml HDPE (Nalgene) sample bottles. Samples were kept cool and in the dark until analysis as soon as possible after arrival. Seawater for trace metal analyses was collected from Niskin bottles attached to the titanium CTD/Rosette system and taken into acid clean LDPE (Nalgene) sample bottles (full details in Birchill et al., 2017). Clean sampling and handling techniques were used. For vertical profiles of phytoplankton <20 μm analysed by flow cytometry, seawater was sampled at 5–13 depth intervals between 2 and 100 m using a rosette of Niskin bottles mounted on a CTD system. The samples were stored at 4°C in the dark until analysis within 2 hr. At a reduced number of stations and depth horizons, additional identification of phytoplankton was carried out via light microscopy.

2.5 | Macronutrient analysis

The micromolar nutrient analysis was carried out using a SEAL Analytical 5-channel (nitrate, nitrite, phosphate, silicate, ammonium) AAIII segmented flow, colorimetric, autoanalyser, using classical proven analytical techniques (Woodward & Rees, 2001). Detection limits for nitrate, nitrite and phosphate were 0.02 μmol/L, and for ammonium was 0.05 μmol/L. The concentration of silicate was always within the detection limit of the analyser. The accuracy of the measurements was 1%–2%. Nitrate and nitrite concentrations were combined and presented as 'nitrate'.

2.6 | Trace metal analysis

Details of trace metal sampling and analysis are provided in Birchill et al. (2017). In brief, trace metal samples were collected following GEOTRACES protocols (Cutter et al., 2017). Dissolved Fe (0.2 μm filtered) was analysed using flow injection with chemiluminescence detection (Floor et al., 2015; Obata, Karatani, & Nakayama, 1993), after spiking with hydrogen peroxide (Lohan, Aguilar-Islas, & Bruland, 2006).
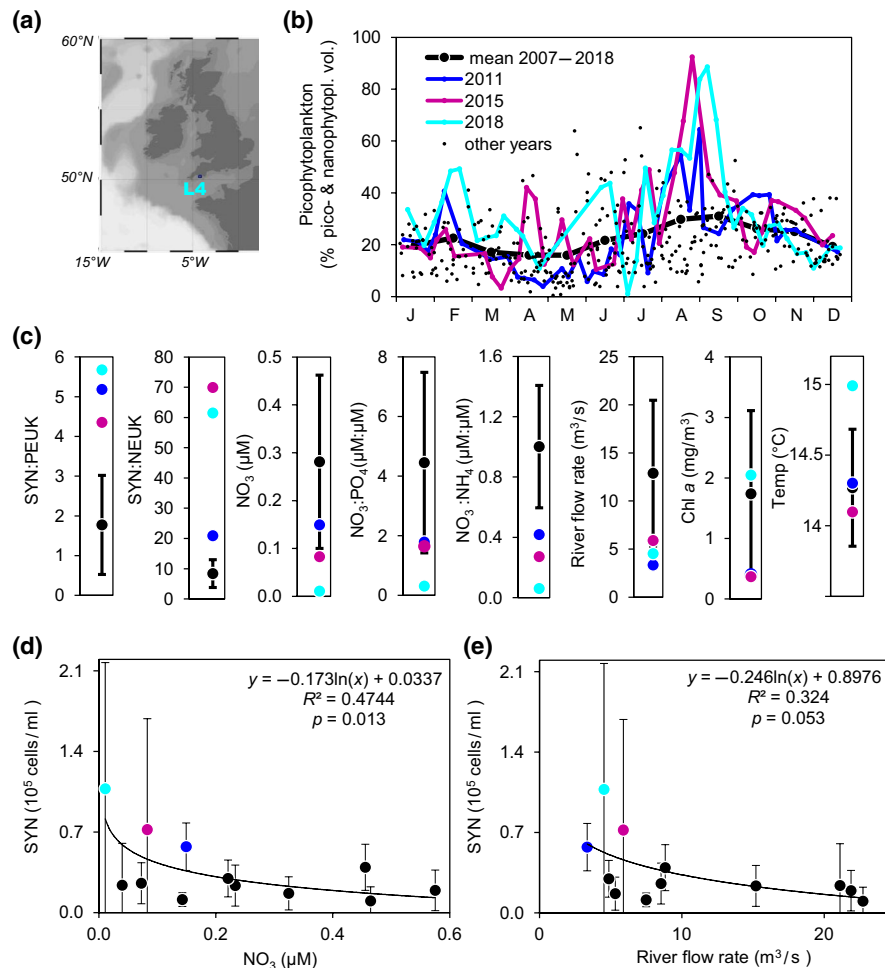
FIGURE 2 Interannual variability in coastal *Synechococcus* abundance is driven by nitrate concentrations and nutrient supply via river outflow. Twelve years of weekly monitoring at a coastal site in the Western English Channel (L4, 2007–2018). (a) Map of the sampling location. (b) The proportion of picophytoplankton in the combined pico- and nanophytoplankton volume (individual values and monthly mean, n = 475). The years 2011, 2015 and 2018 are highlighted as picophytoplankton accounted repeatedly for >50% of the combined pico- and nanophytoplankton volume. (c) Comparison of prevailing environmental conditions during years with high proportions of picophytoplankton (2011, 2015, 2018) and years with low proportions of picophytoplankton (2007, 2008, 2009, 2010, 2012, 2013, 2014, 2016, 2017, mean ± 1 *SD*). For the environmental parameters, the mean value during the stratified period (May–August) is represented, while ratios between picocyanobacteria (*Synechococcus*, SYN) and picoeukaryotes (PEUK) or nanoeukaryotes (NEUK) are based on mean values in August and September, when picophytoplankton is most prominent at this site. Sampling depths: pico- and nanophytoplankton (10 m), nutrients (0 m), Chl *a* (2–50 m integrated), temperature (2–10 m integrated). (d) Annual average nitrate concentration during the stratified period (May–August) as a predictor of the *Synechococcus* abundance in August and September (mean ± 1 *SD*, n ~ 8). (e) Annual average river flow rate during the stratified period (May–August) as a predictor of the *Synechococcus* abundance in August and September (mean ± 1 *SD*, n ~ 8). Together, nitrate concentration and river flow rate explain 61% of the interannual variability in the *Synechococcus* abundance: SYN (cells/ml) = 0.456 − 0.1669 ln river flow rate − 0.1413 ln nitrate concentration. *n* = number of sampling events

2.7 | Flow cytometry analysis

Phytoplankton smaller than ~20 μm were analysed by flow cytometry with distinction between picocyanobacteria (*Synechococcus*), picoeukaryotes and nanoeukaryotes (including coccolitophores, cryptophytes and other nanoeukaryotes). Samples were enumerated using a Becton Dickinson FACSort[TM] flow cytometer (BD) from 2007 until October 2010 and a BD Accuri[TM] C6 flow cytometer since October 2010. Further details of the method are provided in Tarran and Bruun (2015). The median cell volume of each of these categories was calculated from median diameter

measurements by size-fractionating seawater samples through successive polycarbonate membrane filters (Poreticsis®) from 10 μm down to 0.2 μm. A carbon conversion factor of 0.22 pg C/μm^3 was used (Booth, 1988).

2.8 | Light microscopic analysis of phytoplankton

Samples for the enumeration of phytoplankton ≥10 μm were immediately fixed with 2% Lugol's iodine and stored in cool, dark conditions. Taxonomic analysis using light microscopy followed the British

and European standard protocol (BS EN 15204:2006). Mean cell measurements of individual taxa were used to calculate cell biovolume (Olenina et al., 2006) and converted to carbon (pg C/cell) using the equations of Menden-Deuer and Lessard (2000).

3 | RESULTS

3.1 | Combining satellite and CPR time series

To provide the large-scale spatiotemporal context of change, we considered an area of ~2,000 × 1,500 km in the NE Atlantic, centred on shelf regions adjacent to the UK and divided into 16 subareas (Figure 1a). In combination, both satellite and CPR data show similar changes over the longer term (1958–2017) and recently (1997–2017/2018). Between May and August/September, our indices of Chl *a*, diatoms, dinoflagellates and total copepods have all declined, while the proportion of picophytoplankton to total Chl *a* has increased (Figure 1b–i). Unifying features of the trends in both phytoplankton and copepods are first, that they are primarily a summer phenomenon, and second, that they are largely consistent across the 16 subareas that we tested (Figure 1), even though the subareas include shelf and oceanic areas and summer surface temperature varies from ~9°C in the north to ~19°C in the south (Locarnini et al., 2010). The total copepod abundance shows a ~50% decline when comparing median summer values across all 16 subareas in recent years (1997–2017) with those from earlier years since the beginning of the time series (1958–1996; Figure S1). Despite this overall decline in copepod abundance, some species have increased (Figure S1). These are the more carnivorous genera that select for motile food (e.g. *Centropages* spp., Djeghri et al., 2018), whereas more herbivorous genera with a preference for diatoms (e.g. *Oithona* spp., *Para-* and *Pseudocalanus* spp., Djeghri et al., 2018) experienced the strongest decline. The two *Calanus* congeners show opposite trends with the cold-water *C. finmarchicus* being largely replaced by the warm-water *C. helgolandicus* (Figure S1). However, the abundance of the combined offspring of these two species, *Calanus* copepodites I–IV, declined by >60%, in line with the overall loss of copepods across the study area (Figure S1).

3.2 | Interannual differences in the success of picophytoplankton

We used 12 years (2007–2018) of weekly sampling at a coastal monitoring site in the English Channel, L4 (Figure 2a) to encompass seasonal and interannual variability in the abundance of pico- and nanophytoplankton based on flow cytometry data. Here, picophytoplankton accounts on average for 22% of the combined pico- and nanophytoplankton cell volume, with slightly lower values in spring (~16%) and higher values in late summer (~30%, Figure 2b). However, in three of the 12 years (2011, 2015, 2018), picophytoplankton repeatedly contributed >50% and even as much as 90%

to the combined pico- and nanophytoplankton volume (Figure 2b). The 'record' was set in August and September 2018 when the picophytoplankton fraction was >50% in six consecutive weeks. Comparing biotic and abiotic parameters in those 3 years with the mean and standard deviation of the other 9 years, we find (a) high picocyanobacteria-to-picoeukaryote ratios and high picocyanobacteria-to-nanoeukaryote ratios, (b) low NO_3 concentrations and low $NO_3:PO_4$ and $NO_3:NH_4$ ratios, (c) low river flow rates and (d) variable values of Chl *a* and temperature (Figure 2c). This means that the high proportions of picophytoplankton in 2011, 2015 and 2018 were caused by 'blooms' of picocyanobacteria (here *Synechococcus* sp.), while the picoeukaryote abundance was relatively constant. Key conditions that enabled *Synechococcus* to dominate were a combination of low nitrate stocks and low resupply of nutrients via river discharge, and therefore nitrate starvation of the surface waters. Together, nitrate concentration and river flow rate explain 61% of the interannual variability in the *Synechococcus* abundance (Figure 2d,e). The 3 years of high picophytoplankton fractions do not show a matching pattern in any of the other tested parameters (Chl *a*, temperature, stratification, concentration of phosphate, silicate or ammonium). Our findings therefore do not support the hypothesis that temperature is a direct driver of *Synechococcus* abundance (Paulsen et al., 2016) or picophytoplankton fraction (Morán, López-Urrutia, Calvo-Díaz, & Li, 2010). One of the years with high *Synechococcus* abundance at L4 was exceptionally warm (2018), but the other 2 years had average (2011) or below average summer temperatures (2015).

3.3 | *Synechococcus* abundances along a gradient of summer nutrient stress

To further investigate the link between *Synechococcus* abundance and nutrient availability, we explored multiple sampling transects across the shelf and shelf break of the Celtic Sea in spring and summer 2015 (Figure 3a). A key difference between the shelf and the shelf break is the resupply of nutrients to surface waters. The shelf is seasonally stratified; recycled nutrients accumulate below the thermocline and the surface waters become increasingly iron and nitrogen starved (Figure 3b,c; Birchill et al., 2017). In contrast, at the shelf break, internal tides promote the vertical mixing of water masses and therefore the resupply of nutrients to surface waters (Figure 3b,c; Sharples et al., 2009). A comparison of vertical nutrient profiles in spring and summer shows that at the shelf break, a several hundred metre water column acts as a seasonal reservoir to fuel iron, nitrate, silicate and phosphate demands in the euphotic zone (Figure 3c; Figure S2). In line with these regional differences in summer nutrient resupply, *Synechococcus* reached abundances of 2×10^5 cells/ml on the nutrient-starved shelf, while at the shelf break, abundances were an order of magnitude lower even though temperatures were higher (Figure 3b,d). Instead, the shelf break was characterized by higher abundances of diatoms, indicated by cell counts (Table S2) and enhanced $NO_3:Si(OH)_4$ ratios in subsurface waters (Figure 3c).
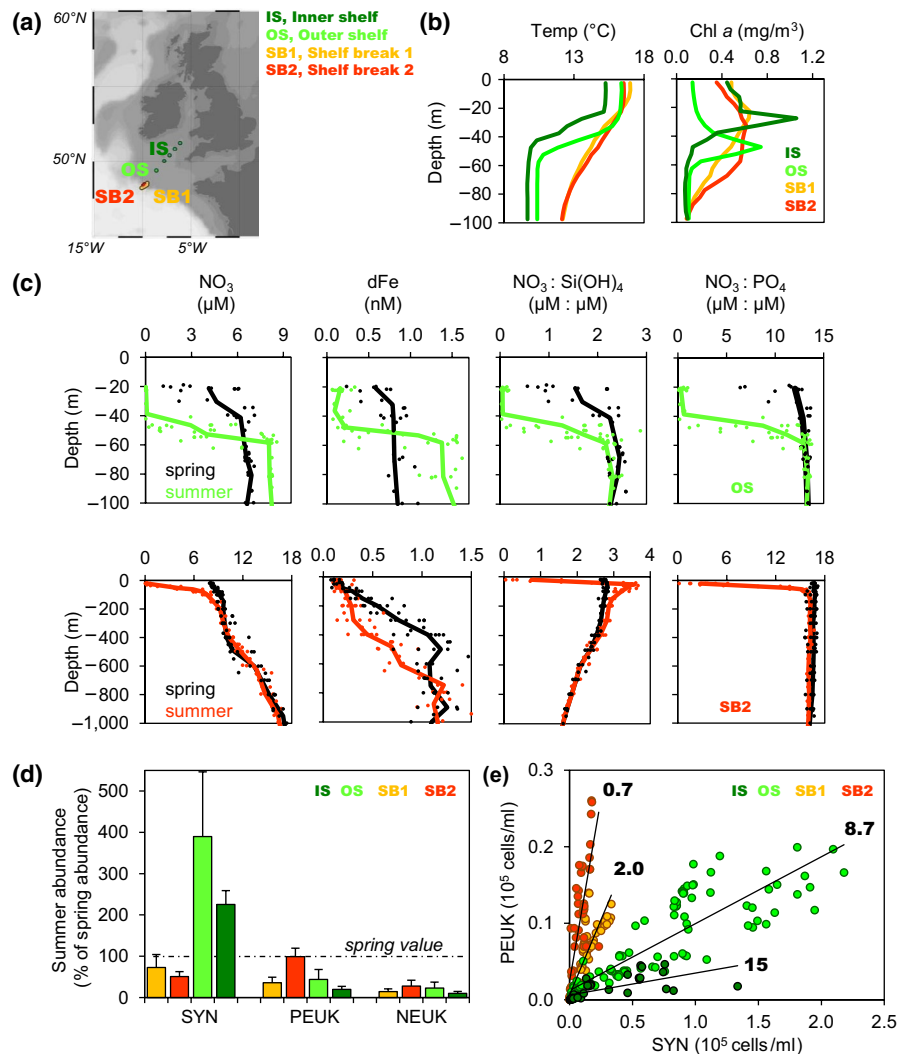
FIGURE 3 Strong stratification and therefore reduced nutrient resupply to surface waters gives *Synechococcus* a competitive edge in temperate shelf waters. Seasonal transects from the inner shelf to the shelf break of the Celtic Sea (spring and summer 2015). (a) Map of the sampling locations: Inner shelf (IS), Outer shelf (OS), Shelf break 1 (SB1), Shelf break 2 (SB2). (b) Average vertical profiles of temperature and Chl *a* at SB1 ($n = 13$), SB2 ($n = 17$), OS ($n = 40$) and IS ($n = 2$) in summer 2015. Based on the maximum vertical temperature difference (ΔTemp, 2–100 m, mean ± 1 *SD*) and potential energy anomaly (PEA, 2–100 m), the vertical stratification at the sampling locations ranked IS > OS>SB1 > SB2. ΔTemp-SB2: 2.1 ± 0.7°C; SB1: 3.1 ± 0.6°C; OS: 5.3 ± 0.7°C; IS: 5.9 ± 0.6°C. PEA-SB2: 135 J/m³; SB1: 138 J/m³; OS: 174 J/m³; IS: 184 J/m³. (c) Average vertical profiles of nitrate, dissolved iron (dFe) and macronutrient ratios (median and individual values) at OS and SB2 in spring 2015 (OS, SB2: $n = 7$) and summer 2015 (OS: $n = 14$, SB2: $n = 7$). Vertical profiles of $Si(OH)_4$ and PO_4 are given in Figure S2. $n =$ number of sampling events. (d) Abundance of phytoplankton groups in summer compared to spring (mean ± 1 *SD*). *Synechococcus* (SYN), picoeukaryotes (PEUK), nanoeukaryotes (NEUK). (e) Summer *Synechococcus*-to-picoeukaryote ratios, individual values and average (bold), at different sampling locations. Data derived from the upper 100 m water column. SB1 ($n = 8$), SB2 ($n = 7$), OS ($n = 11$), IS ($n = 4$). $n =$ number of stations

Depth-integrated Chl *a* concentrations were about twice as high at the shelf break compared to the shelf (Figure 3b), confirming the overall higher productivity of this region (Sharples et al., 2009).

3.4 | Traits that allow *Synechococcus* to outcompete picoeukaryotes

During our studies, *Synechococcus* and picoeukaryotes were of nearly identical size both at the monitoring site L4 (1.7 vs. 1.8 µm)

and in the Celtic Sea (1.3 vs. 1.4 µm; Table S3). This allows us to examine traits, other than small size, that give *Synechococcus* a competitive advantage under low nutrient concentrations. The L4 seasonal cycle of the *Synechococcus*-to-picoeukaryote ratio shows a characteristic sine wave (Figure 4a), which means that there are times when picoeukaryotes outcompete *Synechococcus* and vice versa. Starting with a winter 1:1 ratio, picoeukaryotes become increasingly successful when growth conditions improve in spring (enhanced daylight, sufficient nutrient availability; Figure S3), while from mid-summer onwards, exhausted nutrient
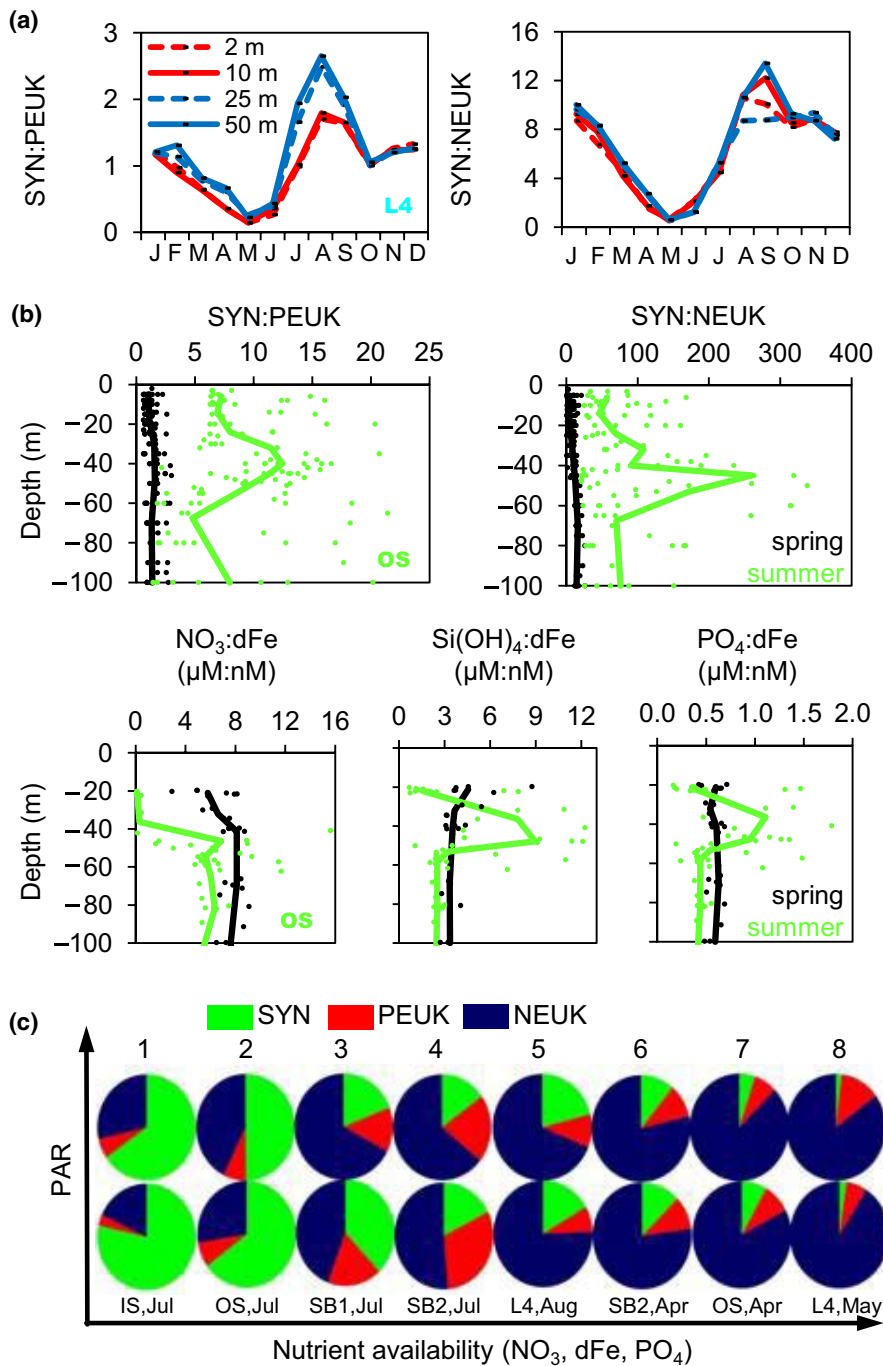
FIGURE 4 Traits that enable *Synechococcus* to outcompete similar size picoeukaryotes during nutrient shortage: Efficient acquisition of light and iron in subsurface waters. (a) Seasonal cycle of *Synechococcus*-to-picoeukaryote ratios (SYN:PEUK) and *Synechococcus*-to-nanoeukaryote ratios (SYN:NEUK; monthly median, n ~ 48) at the coastal monitoring site L4. (b) Analogy in the vertical profiles of SYN:PEUK, SYN:NEUK and macronutrient-to-dissolved iron ratios at OS in summer 2015. For all parameters, individual values and the median are presented (a few data points are beyond the plotted scale). Number of sampling events: SYN:PEUK; SYN:NEUK spring (n = 15), summer (n = 11); macronutrients and dissolved iron spring (n = 7), summer (n = 14). (c) Pico- and nanophytoplankton community composition (% biovolume) along a nutrient irradiance gradient. High PAR values (top) refer to ~10 m water depth, low PAR values (bottom) to the subsurface Chl *a* maximum or 40–50 m water depth. Information on microscopically counted diatoms and dinoflagellates is given in Table S2a

pools give *Synechococcus* an advantage and the *Synechococcus*-to-picoeukaryote ratio rises to >2. A similar seasonal cycle is found at a second monitoring site in the English Channel and for the *Synechococcus*-to-nanoeukaryotes ratio (Figure 4a; Figure S4). Across the Celtic Sea shelf break and shelf, *Synechococcus*-to-picoeukaryote ratios rose from 0.7 to 15 as the surface water became increasingly stratified (Figure 3b,e), which reflects their superior abilities to outcompete picoeukaryotes under nutrient shortage.

Based on our data, two traits can be identified that likely contribute to *Synechococcus*' success in nutrient-starved waters. First, *Synechococcus* cope better with low light levels than co-occurring

pico- or nanoeukaryotes. This is seen in the enhanced *Synechococcus*-to-picoeukaryote and *Synechococcus*-to-nanoeukaryotes ratios in deeper water (25–80 m) at L4 and the Celtic Sea (Figure 4a,b). Another prerequisite for photosynthesis at low irradiance is a high affinity to iron, indicated by the major increase in Fe:N and Fe:P ratios of phytoplankton when grown under low irradiance (Figure S5 adapted from Finkel et al., 2006). In the Celtic Sea, enhanced macronutrient-to-iron ratios [NO_3:dFe, $Si(OH)_4$:dFe, PO_4:dFe] occur in subsurface waters of ~20 to 60 m depth where *Synechococcus* account for up to 80% of the combined pico- and nanophytoplankton volume (Figure 4b). This implies that *Synechococcus* is efficient at iron uptake.

4 | DISCUSSION

4.1 | The *Synechococcus* 'strategy': Structural investment for sustained resource acquisition

Our study shows that *Synechococcus* can best outcompete pico- and nanoeukaryotes in subsurface waters where light levels are as low as 2% surface irradiance (Figure 4a,b; Figure S6). Occupying these darker waters enhances the chances of nutrient uptake near the pycnocline; however, it requires efficient harvesting of both light and iron to sustain photosynthesis (Finkel et al., 2006).

Compared to the dominant picoeukaryote in the study area, the prasinophyte *Micromonas pusilla* (Not et al., 2004), *Synechococcus'* suite of light-harvesting pigments is superior for light absorption in subsurface coastal waters (Figure 5). *Synechococcus* populations from the Western English Channel are capable of Type IV chromatic acclimation (Humily et al., 2014), which means that they can change the ratio of blue light-absorbing phycourobilin (A_{max} = 495 nm) versus green light-absorbing phycoerythrobilin (A_{max} = 550 nm) depending on the ambient light colour (Grébert et al., 2018). In contrast, chlorophyll *b*, the light-harvesting pigment of *M. pusilla* has its maximum absorption in darker blue light (A_{max} = 480 nm; Kunugi et al., 2016), which is less suitable in subsurface coastal waters where green light prevails (Figure 5).

Other studies have shown that, in contrast to their oceanic counterparts, coastal *Synechococcus* are well adapted to fluctuating iron concentrations (Mackey et al., 2015; Palenik et al., 2006). Their ability to use or even produce strong iron chelators (e.g. siderophores; Hutchins, Witter, Butler, & Luther, 1999; Ito & Butler, 2005; Wilhelm & Trick, 1994) and their enhanced iron storage capacities (Mackey et al., 2015) may give *Synechococcus* a competitive edge over picoeukaryotes (Figure 5). Laboratory experiments have shown that iron uptake rates of the siderophore-producing coastal Atlantic isolate *Synechococcus* PCC7002 are ~3 times higher than those of a non-siderophore-producing oceanic strain (Lis, Kranzler, Keren, & Shaked, 2015). However, it is currently unknown how widespread siderophore production is among coastal picocyanobacteria (Hopkinson & Morel, 2009).

On the downside for *Synechococcus*, both the phycobilisome-based light-harvesting system and siderophore transport systems are costly cell structures (Lis et al., 2015; Ting Rocap, King, & Chisholm, 2002), which may explain the exceptionally high nitrogen demand and relatively low growth rates of coastal *Synechococcus* (Figure 5). For a given carbon content, the *Synechococcus* PCC7002 strain contains 64% more nitrogen than *M. pusilla* (Blanco-Ameijeiras et al., 2018; Maat, Crawfurd, Timmermans, & Brusaard, 2014). In line with this, the protein investment for the phycobilisome-based light-harvesting system of *Synechococcus* is >3 times higher than for the chlorophyll *a/b*-based antennae of green algae (Ting, Rocap, King, & Chisholm, 2002). A less demanding structural composition may enable *M. pusilla* to grow about twice as fast as *Synechococcus* under nutrient replete conditions (Marañón et al., 2013).

Slow grow rates make *Synechococcus* vulnerable to grazing control. In the laboratory, *Synechococcus* growth shows a positive relationship to temperature (Agawin, Duarte, & Agustí, 1998), but at L4, their abundances reach the annual minimum not in the coldest month February, but in May when their mixotrophic grazers (Tsai, Chiang, Chan, Lin, & Chang, 2007) find ideal growth conditions. Similar size picoeukaryotes seem to be less affected by grazing, as the low *Synechococcus*-to-picoeukaryote ratios in May indicate. Likewise, at the nutrient-replete shelf break of the Celtic Sea, *Synechococcus* remained under grazing control during summer, even though temperatures were higher than on the shelf.

Overall, we suggest that the strategy of coastal *Synechococcus* consists of high structural investments for sustained resource acquisition (light, nutrients), with the trade-off of low growth rates and high vulnerability to grazing. This strategy pays off when competing pico- and nanoeukaryotes are severely nutrient limited and their grazing pressure eases.

4.2 | *Synechococcus* are extending their global distribution

Picocyanobacteria of the genus *Synechococcus* are among the most important and widespread marine primary producers (Flombaum et al., 2013). This is enabled by the existence of >20 genetically distinct clades, some of which inhabit cold, mesotrophic waters, others warm, oligotrophic open ocean or sites with permanently low iron availability (Paulsen et al., 2016; Sohm et al., 2016). Some strains are specifically adapted to the dynamic coastal environments, for example, via their pigment types and capacity to sense and respond to changes in iron availability (Grébert et al., 2018; Mackey et al., 2015; Palenik et al., 2006).

Niche models project a 14% increase in global cell numbers of *Synechococcus* by the end of the 21st century, which involves their spatial expansions (Flombaum et al., 2013). While all four of their model projections agree that these increases will occur in low latitudes, some models project also up to 50% increase in *Synechococcus* numbers for mid- and higher latitudes (40–60°N; Flombaum et al., 2013). Our study shows that, already in the present day, *Synechococcus* can dominate the phytoplankton biomass in temperate shelf and coastal areas if certain conditions are met. Crucial are not high temperatures per se, but rather a reduced resupply of nutrients to surface waters. We identify intense stratification and low river discharge as conditions that can lead to this nutrient starvation. Both macronutrients and dissolved iron are affected by this lack of resupply, with iron stress only recently recognized to extend onto the NW European shelf (Birchill et al., 2017, 2019). Our process studies suggest that *Synechococcus* is highly competitive under nitrogen–iron colimitation, a state of nutrient limitation that is pervasive throughout ~50% of the global surface ocean (Browning et al., 2017).

Extended periods of water column stratification, droughts and heat waves are predicted for future summers across the NE Atlantic (Holt et al., 2016; IPCC, 2019; Yool, Popova, & Coward, 2016). We
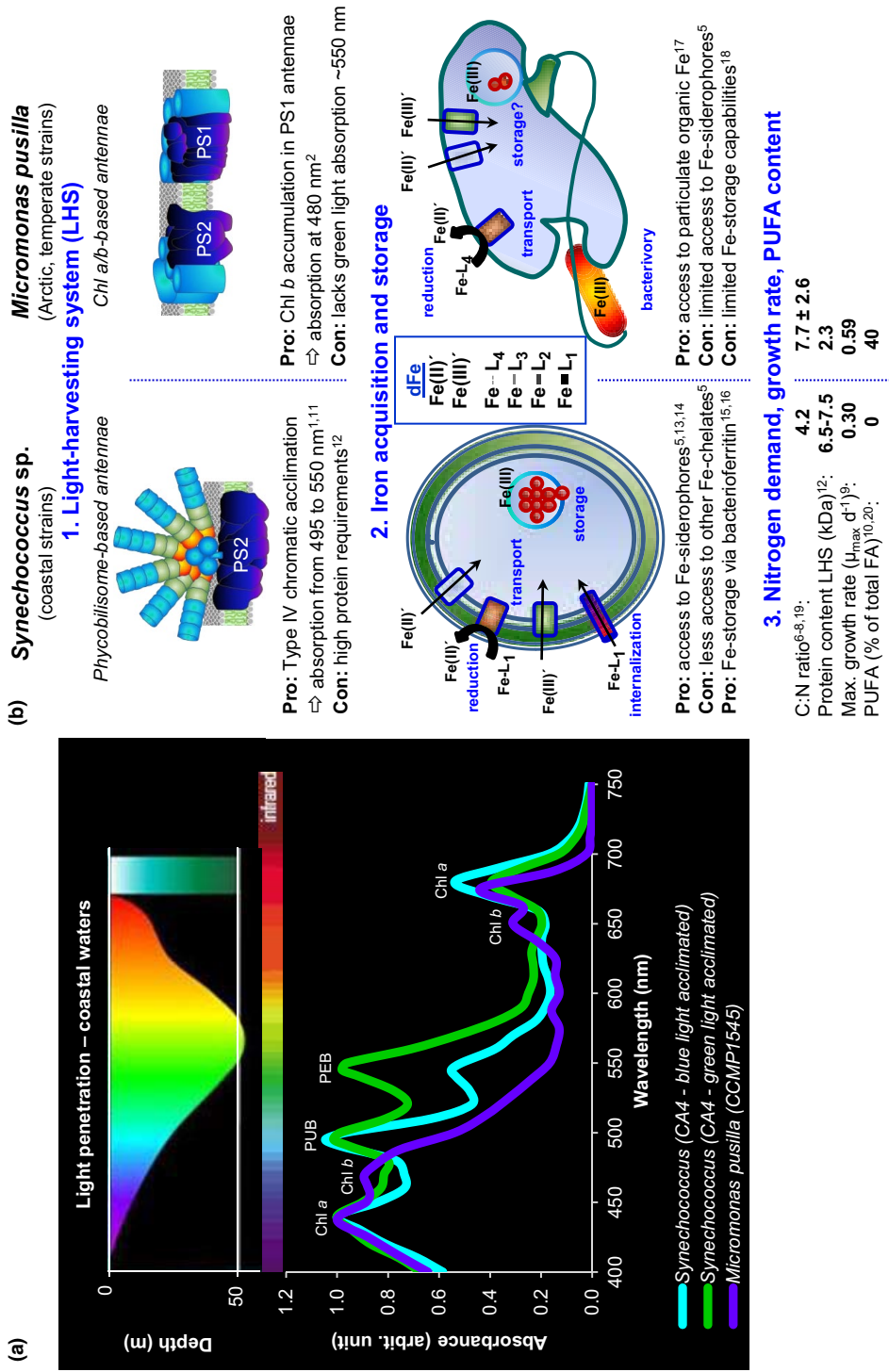
FIGURE 5 Traits and trade-offs in *Synechococcus* compared to an equal-sized picoeukaryote (*Micromonas pusilla*): High structural investment enables sustained resource acquisition (light, iron) under shortage, but prevents fast growth when resources are plentiful. (a) Comparison between light penetration in coastal waters and the absorption spectra of *Synechococcus* (two acclimation stages)[1] and *M. pusilla*.[2] The absorption spectra were normalized to a value of 1 at the Chl *a* peak (A_{max} = 440 nm). PEB, phycoerythrobilin; PUB, phycourobilin. *Synechococcus* populations that are capable of Type IV chromatic acclimation (*CA4*), that is, to change their PUB:PEB ratio depending on the ambient light colour, have been reported from the Western English Channel[3] (WEC). *M. pusilla* has been identified as the dominant picoeukaryote in the WEC[4]. (b) Differences between coastal *Synechococcus* and *M. pusilla* in terms of their (1) light-harvesting strategies, (2) iron acquisition and storage and (3) nitrogen demand, growth rate and content of polyunsaturated fatty acids (PUFA). Up to 99% of the dissolved Fe (dFe) in seawater is complexed by naturally occurring organic ligands (L). These ligands can facilitate or impede iron uptake by phytoplankton depending on their identity: L_1—strong ligands (e.g. siderophores), L_2—moderate ligands (e.g. humics, biological degradation/excretion products), L_3; L_4—weak ligands (e.g. saccharides). Prokaryotes and eukaryotes seem to differ in their efficiency to access these various iron chelates[5]. Compared to other phytoplankton species, *Synechococcus* has a high nitrogen demand[6–8] and low growth rates.[9] Like all cyanobacteria, *Synechococcus* lacks PUFA[1], which are an essential diet component for higher trophic levels. The given C:N ratios derived from nutrient replete cultures. The protein investment is normalized to one tetrapyrrole of the light-harvesting system (LSH). 1. Six et al. (2007). 2. Kunugi et al. (2016). 3. Humily et al. (2014). 4. Not et al. (2004). 5. Hutchins et al. (1999). 6. Geider and La Roche (2002). 7. Bertilsson, Berglund, Karl, & Chisholm (2003). 8. Blanco-Ameijeiras et al. (2018). 9. Marañón et al. (2013). 10. Patil et al. (2007). 11. Grébert et al. (2018). 12. Ting et al. (2002). 13. Lis et al. (2015). 14. Ito and Butler (2005). 15. Mackey et al. (2015). 16. Palenik et al. (2006). 17. McKie-Krisberg and Sanders (2014). 18. Sutak et al. (2012). 19. Maat et al. (2014). 20. Jónasdóttir (2019)

suggest that these conditions will increasingly benefit the advance of *Synechococcus* into shelf areas.

4.3 | Implications for energy flow through pelagic food webs

Zooplankton such as copepods are considered beacons of climate change (Richardson, 2008) and can be more sensitive indicators than the environmental variables themselves, due to their non-linear responses that can amplify subtle environmental changes (Taylor, Allen, & Clark, 2002). Moreover, it has been suggested that trophic amplification can lead to significantly larger changes in fishery resources than implied by net primary production changes alone (Chust et al., 2014). In this respect, we have to interpret the overall ~50% decline in copepod abundance over the last 60 years (Figure S1) and the large spatial extent of this decline (Figure 1) as clear indications that growth conditions for zooplankton in the NE Atlantic have changed (time series: 1958–1996) and are changing (time series: 1997–2017).

Biogeographical and phenological shifts due to increasing temperature are known to be occurring in the north Atlantic (Beaugrand et al., 2002). However, alternative (non-mutually incompatible) mechanisms have also been proposed, namely declining primary production as a cause of the copepod decline in the North Sea (Capuzzo et al., 2017). Based on an extensive network of time series, Bedford et al. (2020) show that this long-term copepod decline extends from inshore to offshore areas right across the NW European shelf. Our study spans an even larger area and by detailing the species composition and seasonal timing of the copepod decline, we shed light on the potential causes. First, the copepod decline is observed across the whole NE Atlantic and fringing shelves; too large an area to be solely explainable by the observed magnitude of range shifts (Chivers, Walne, & Hays, 2017). Second, it occurs for both large and small copepod species and across those with different temperature preferences. Third, it is a summer phenomenon, at the time when the food composition has changed the most (Figure 1). We conclude that, in addition to the direct effects of rising temperature, significant changes are occurring in the food environment of these copepods.

Even though *Synechococcus* can reach near-bloom concentrations in subsurface layers (Chl a ~ 1 mg/m^3, Figure 3b), this biomass is of limited use for copepods as they cannot capture cells <5 μm efficiently (Kiørboe, 2008). Moreover, like all cyanobacteria, *Synechococcus* lack biomolecules such as omega-3 polyunsaturated fatty acids and sterols (Jónasdóttir, 2019; Patil, Källqvist, Olsen, Vogt, & Gislrød, 2007; Ruess & Müller-Navarra, 2019). These compounds are essential for both copepods and fish to acquire from their diet in order to sustain egg production and growth. Thus, under summer conditions, the 'classical food chain' from diatoms or dino-flagellates via copepods to fish is severely reduced, giving way to the 'microbial food web' from *Synechococcus* via flagellates and ciliates to copepods and fish. However, this microbial pathway is less efficient, both because of the increased number of trophic steps and the lower nutritional quality of the main primary producer (Figure S7).

While we highlight the role of diminishing food quality, other factors contribute to summer becoming an increasingly stressful period of the year for pelagic consumers. These include a spring bloom that occurs earlier in the year (here indicated by a Chl a increase in April and decrease in May, Figure 1b) and the overall decrease in phytoplankton biomass in summer (Figure 1b). Together, these all lengthen the summer period of low food quality and quantity for zooplankton. Winter food shortage is easier manageable due to low temperatures and therefore low basal metabolism, but respiration costs are high in summer and prolonged lack of food at this time of year has more adverse effects. Such a nutrition-related mismatch during summer will increasingly challenge temperate shelf and coastal areas to maintain their historically important food chains.

DATA AVAILABILITY STATEMENT
Data are available upon request from the authors.

ORCID

Katrin Schmidt https://orcid.org/0000-0002-6488-623X
Antony J. Birchill https://orcid.org/0000-0002-1453-5781
Angus Atkinson https://orcid.org/0000-0002-5931-4325
Robert J. W. Brewin https://orcid.org/0000-0001-5134-8291
James R. Clark https://orcid.org/0000-0002-1924-5871
David G. Johns https://orcid.org/0000-0003-3270-6764
Maeve C. Lohan https://orcid.org/0000-0002-5340-3108
Angela Milne https://orcid.org/0000-0002-3304-8962
Silvia Pardo https://orcid.org/0000-0001-9773-0058
Luca Polimene https://orcid.org/0000-0002-3549-6937

Tim J. Smyth (iD) https://orcid.org/0000-0003-0659-1422
Glen A. Tarran (iD) https://orcid.org/0000-0003-3695-5151
Claire E. Widdicombe (iD) https://orcid.org/0000-0002-1688-0212
E. Malcolm S. Woodward (iD) https://orcid.
org/0000-0002-7187-6689
Simon J. Ussher (iD) https://orcid.org/0000-0001-6724-9212

REFERENCES

Agawin, N. S. A., Duarte, C. M., & Agustí, S. (1998). Growth and abundance of *Synechococcus* sp. in a Mediterranean Bay: Seasonality and relationship with temperature. *Marine Ecology Progress Series*, *170*, 45–53. https://doi.org/10.3354/meps170045

Agawin, N. S. R., Duarte, C. M., & Agustí, S. (2000). Nutrient and temperature control of the contribution of picoplankton to phytoplankton biomass and production. *Limnology and Oceanography*, *45*, 591–600. https://doi.org/10.4319/lo.2000.45.3.0591

Agirbas, E., Martinez-Vicente, V., Brewin, R. J. W., Racault, M.-F., Airs, R. L., & Llewellyn, C. A. (2015). Temporal changes in total and size-fractionated chlorophyll-a in surface waters of three provinces in the Atlantic Ocean (September to November) between 2003 and 2010. *Journal of Marine Systems*, *150*, 56–65. https://doi.org/10.1016/j.jmarsys.2015.05.00

Beaugrand, G., Brander, K. M., Lindley, J. A., Souissi, S., & Reid, P. C. (2003). Plankton effect on cod recruitment in the North Sea. *Nature*, *426*, 661–664. https://doi.org/10.1038/nature02164

Beaugrand, G., Reid, P. C., Ibanez, F., Lindley, J. A., & Edwards, M. (2002). Reorganisation of North Atlantic marine copepod diversity and climate. *Science*, *296*, 1692–1694. https://doi.org/10.1126/science.1071329

Bedford, J., Ostle, C., Johns, D. G., Atkinson, A., Best, M., Bresnan, E., … McQuatters-Gollop, A. (2020). Lifeform indicators reveal large-scale shifts in plankton across the North-West European shelf. *Global Change Biology*, *00*, 1–16. https://doi.org/10.1111/gcb.15066

Bertilsson, S., Berglund, O., Karl, D. M., & Chisholm, S. W. (2003). Elemental composition of marine *Prochlorococcus* and *Synechococcus*: Implications for the ecological stoichiometry of the sea. *Limnology and Oceanography*, *48*, 1721–1731. https://doi.org/10.4319/lo.2003.48.5.1721

Birchill, A. J., Hartner, N. T., Kunde, K., Siemering, B., Daniels, C., González-Santana, D., … Lohan, M. C. (2019). The eastern extent of seasonal iron limitation in the high latitude North Atlantic Ocean. *Scientific Reports*, *9*, 1435. https://doi.org/10.1038/s41598-018-37436-3

Birchill, A. J., Milne, A., Woodward, E. M. S., Harris, C., Annett, A., Rusiecka, D., … Lohan, M. C. (2017). Seasonal iron depletion in temperate shelf seas. *Geophysical Research Letters*, *44*, 8987–8996. https://doi.org/10.1002/2017GL073881

Blanco-Ameijeiras, S., Moisset, S. A. M., Trimborn, S., Campbell, D. A., Heiden, J. P., & Hassler, C. S. (2018). Elemental stoichiometry and photophysiology regulation of *Synechococcus* sp. PCC7002 under increasing severity of chronic iron limitation. *Plant and Cell Physiology*, *59*, 1803–1816. https://doi.org/10.1093/pcp/pcy097

Booth, B. C. (1988). Size classes and major taxonomic groups of phytoplankton at two locations in the subarctic Pacific Ocean in May and August, 1984. *Marine Biology*, *97*, 275–286. https://doi.org/10.1007/BF00391313

Bopp, L., Resplandy, L., Orr, J. C., Doney, S. C., Dunne, J. P., Gehlen, M., … Vichi, M. (2013). Multiple stressors of ocean ecosystems in the 21st century: Projections with CMIP5 models. *Biogeosciences*, *10*, 6225–6245. https://doi.org/10.5194/bg-10-6225-2013

Brewin, R. J. W., Ciavatta, S., Sathyendranath, S., Jackson, T., Tilstone, G., Curran, K., … Raitsos, D. E. (2017). Uncertainty in ocean-color estimates of chlorophyll for phytoplankton groups. *Frontiers in Marine Science*, *4*, 104. https://doi.org/10.3389/fmars.2017.00104

Brewin, R. J. W., Hirata, T., Hardman-Mountford, N. J., Lavender, S., Sathyendranath, S., & Barlow, R. (2012). The influence of the Indian Ocean Dipole on interannual variations in phytoplankton size structure as revealed by Earth Observation. *Deep-Sea Research II*, *77–80*, 117–127. https://doi.org/10.1016/j.dsr2.2012.04.009

Browning, T. J., Achterberg, E. P., Rapp, I., Engel, A., Bertrand, E. M., Tagliabue, A., & Moore, C. M. (2017). Nutrient co-limitation at the boundary of an oceanic gyre. *Nature*, *551*, 242–246. https://doi.org/10.1038/nature24063

Capuzzo, E., Lynam, C. P., Barry, J., Stephens, D., Forster, R. M., Greenwood, N., … Engelhard, G. H. (2017). A decline in primary production in the North Sea over 25 years, associated with reductions in zooplankton abundance and fish stock recruitment. *Global Change Biology*, *24*, 352–364. https://doi.org/10.1111/gcb.13916

Chassot, E., Bonhommeau, S., Dulvy, N. K., Mélin, F., Watson, R., Gascuel, D., & Le Pape, O. (2010). Global marine primary production constrains fishery catches. *Ecology Letters*, *13*, 495–505. https://doi.org/10.1111/j.1461-0248.2010.01443.x

Chisholm, S. W. (1992). Phytoplankton size. In P. G. Falkowski, A. D. Woodhead, & K. Vivirito (Eds.), *Primary productivity and biogeochemical cycles in the sea. Environmental science research* (Vol. 43, pp. 213–237). Boston, MA: Springer. https://doi.org/10.1007/978-1-4899-0762-2_12

Chivers, W., Walne, A., & Hays, G. (2017). Mismatch between marine plankton range movements and the velocity of climate change. *Nature Communications*, *8*, 14434. https://doi.org/10.1038/ncomms14434

Chust, G., Allen, J. I., Bopp, L., Schrum, C., Holt, J., Tsiaras, K., … Irigoien, X. (2014). Biomass changes and trophic amplification of plankton in a warmer ocean. *Global Change Biology*, *20*, 2124–2139. https://doi.org/10.1111/gcb.12562

CMEMS. (2018).Information document for ocean colour Atlantic and Arctic observation products, CMEMS-OC-QUID-009-066-067-068-069-088-091, issue 1.6 (May 2018). Retrieved from http://marine.copernicus.eu/documents/QUID/CMEMS-OC-QUID-009-066-067-068-069-088-091.pdf

Cutter, G., Casciotti, K., Croot, P., Geibert, W., Heimbürger, L.-E., Lohan, M., … van de Flierdt, T. (2017). *Sampling and sample-handling protocols for GEOTRACES cruises*. Version 3, August 2017. Toulouse, France: GEOTRACES International Project Office, 139 pp. & Appendices. https://doi.org/10.25607/OBP-2

Desmit, X., Nohe, A., Borges, A. V., Prins, T., De Cauwer, K., Lagring, R., … Sabbe, K. (2020). Changes in chlorophyll concentration and phenology in the North Sea in relation to de-eutrophication and sea surface warming. *Limnology and Oceanography*, *65*, 828–847. https://doi.org/10.1002/lno.11351

Djeghri, N., Atkinson, A., Fileman, E. S., Harmer, R. A., Widdicombe, C. E., McEvoy, A. J., … Mayor, D. J. (2018). High prey-predator size ratios and unselective feeding in copepods: A seasonal comparison of five species with contrasting feeding modes. *Progress in Oceanography*, *165*, 63–74. https://doi.org/10.1016/j.pocean.2018.04.013

Dutkiewicz, S., Scott, J. R., & Follows, M. J. (2013). Winners and losers: Ecological and biogeochemical changes in a warming ocean. *Global Biogeochemical Cycles*, *27*, 463–477. https://doi.org/10.1002/gbc.20042

Finkel, Z. V., Quigg, A., Raven, J. A., Reinfelder, J. R., Schofield, O. E., & Falkowski, P. G. (2006). Irradiance and the elemental stoichiometry of marine phytoplankton. *Limnology and Oceanography*, *51*, 2690–3270. https://doi.org/10.4319/lo.2006.51.6.2690

Finkel, Z. V., Sebbo, J., Feist-Burkhardt, S., Irwin, A. J., Katz, M. E., Schofield, O. M. E., … Falkowski, P. G. (2007). A universal driver of macroevolutionary change in the size of marine phytoplankton over the Cenozoic. *Proceedings of the National Academy of Sciences*

of the United States of America, *104*, 20416–20420. https://doi.org/10.1073/pnas.0709381104

Flombaum, P., Gallegos, J. L., Gordillo, R. A., Rincón, J., Zabala, L. L., Jiao, N., ... Martiny, A. C. (2013). Present and future global distributions of the marine cyanobacteria *Prochlorococcus* and *Synechococcus*. *Proceedings of the National Academy of Sciences of the United States of America*, *110*, 9824–9829. https://doi.org/10.1073/pnas.1307701110

Floor, G. H., Clough, R., Lohan, M. C., Ussher, S. J., Worsfold, P. J., & Quétel, C. R. (2015). Combined uncertainty estimation for the determination of the dissolved iron amount content in seawater using flow injection with chemiluminescence detection. *Limnology and Oceanography: Methods*, *13*, 673–686. https://doi.org/10.1002/lom3.10057

Friedland, K. D., Mouw, C. B., Asch, R. G., Ferreira, A. S. A., Henson, S., Hyde, K. J. W., ... Brady, D. C. (2018). Phenology and time series trends of the dominant seasonal phytoplankton bloom across global scales. *Global Ecology and Biogeography*, *27*, 551–569. https://doi.org/10.1111/geb.12717

Geider, R. J., & La Roche, J. (2002). Redfield revisited: Variability of C:N:P in marine microalgae and its biochemical basis. *European Journal of Phycology*, *37*, 1–17. https://doi.org/10.1017/S0967026201003456

Grébert, T., Dore, H., Partensky, F., Farrant, G. K., Boss, E. S., Picheral, M., ... Garczarek, L. (2018). Light color acclimation is a key process in the global ocean distribution of *Synechococcus cyanobacteria*. *Proceedings of the National Academy of Sciences of the United States of America*, *115*, E2010–E2019. https://doi.org/10.1073/pnas.1717069115

Greenberg, P. (2018). *The omega principle: Seafood and the quest for a long life and a healthier planet*. London, UK: Penguin Press, 282 pp. ISBN 978-1-59420-634-4.

Holt, J., Schrum, C., Cannaby, H., Daewel, U., Allen, I., Artioli, Y., ... Wakelin, S. (2016). Potential impacts of climate change on the primary production or regional seas: A comparative analysis of five European seas. *Progress in Oceanography*, *140*, 91–115. https://doi.org/10.1016/j.pocean.2015.11.004

Holt, J. S., Wakelin, S., Lowe, J., & Tinker, J. (2010). The potential impacts of climate change on the hydrography of the northwest European continental shelf. *Progress in Oceanography*, *86*, 361–379. https://doi.org/10.1016/j.pocean.2010.05.003

Hopkinson, B. M., & Morel, F. M. M. (2009). The role of siderophores in iron acquisition by photosynthetic marine microorganisms. *BioMetals*, *22*, 659–669. https://doi.org/10.1007/s10534-009-9235-2

Humily, F., Farrant, G. K., Marie, D., Partensky, F., Mazard, S., Perennou, M., ... Garczarek, L. (2014). Development of a targeted metagenomic approach to study a genomic region involved in light harvesting in marine *Synechococcus*. *FEMS Microbiology Ecology*, *88*, 231–249. https://doi.org/10.1111/1574-6941.12285

Hutchins, D. A., Witter, A. E., Butler, A., & Luther, G. W. (1999). Competition among marine phytoplankton for different chelated iron species. *Nature*, *400*, 858–861. https://doi.org/10.1038/23680

IPCC. (2019). Summary for policymakers. In H.-O. Pörtner, D. C. Roberts, V. Masson-Delmotte, P. Zhai, M. Tignor, E. Poloczanska, K. Mintenbeck, M. Nicolai, A. Okem, J. Petzlod, B. Rama, & N. Weyer (Eds.), *IPPC special report on the ocean and cryosphere in a changing climate*, in press, 36 pp.

Ito, Y., & Butler, A. (2005). Structure of synechobactins, new siderophores of the marine cyanobacterium *Synechococcus* sp. PCC 7002. *Limnology and Oceanography*, *50*, 1918–1923. https://doi.org/10.4319/lo.2005.50.6.1918

Johns, D. G. (2019). Continuous Plankton Recorder data: diatoms (doi 10.7487/2019.224.1.1219), dinoflagellates (doi 10.7487/2019.261.1.1231), copepods (doi 10.7487/2019.169.1.1200; doi 10.7487/2019.197.1.1213).

Jónasdóttir, S. H. (2019). Fatty acid profiles and production in marine plankton. *Marine Drugs*, *17*, 151. https://doi.org/10.3390/md17030151

Kiørboe, T. (2008). *A mechanistic approach to plankton ecology*. Princeton, NJ: Princeton University Press. ISBN 9780691134222.

Kunugi, M., Satoh, S., Ihara, K., Shibata, K., Yamagishi, Y., Kogame, K., ... Tanaka, A. (2016). Evolution of green plants accompanied changes in light-harvesting systems. *Plant and Cell Physiology*, *57*, 1231–1243. https://doi.org/10.1093/pcp/pcw071

Lis, H., Kranzler, C., Keren, N., & Shaked, Y. (2015). A comparative study of iron uptake rates and mechanisms amongst marine and freshwater cyanobacteria: Prevalence of reductive iron uptake. *Life*, *5*, 841–860. https://doi.org/10.3390/life5010841

Locarnini, R. A., Mishonov, A. V., Antonov, J. I., Boyer, T. P., Garcia, H. E., Baranova, O. K., ... Johnson, D. R. (2010). *World ocean atlas 2009, volume 1: Temperature*. In S. Levitus (Ed.). NOAA Atlas NESDIS 68. Washington, DC: U.S. Government Printing Office, 184 pp. Retrieved from http://www.nodc.noaa.gov/OC5/indprod.html

Lohan, M. C., Aguilar-Islas, A. M., & Bruland, K. W. (2006). Direct determination of iron in acidified (pH 1.7) seawater samples by flow injection analysis with catalytic spectrophotometric detection: Application and intercomparison. *Limnology and Oceanography: Methods*, *4*, 164–171. https://doi.org/10.4319/lom.2006.4.164

Maat, D. S., Crawford, K. J., Timmermans, K. R., & Brusaard, C. P. D. (2014). Elevated CO_2 and phosphate limitation favour *Micromonas pusilla* through stimulate growth and reduced viral impact. *Applied and Environmental Microbiology*, *80*(10), 3119–3127. https://doi.org/10.1128/AEM.03639-13

Mackey, K. R. M., Post, A. F., McIlvin, M. R., Cutter, G. A., John, S. G., & Saito, M. A. (2015). Divergent responses of Atlantic coastal and oceanic *Synechococcus* to iron limitation. *Proceedings of the National Academy of Sciences of the United States of America*, *112*, 9944–9949. https://doi.org/10.1073/pnas.1509448112

Marañón, E., Cermeño, P., López-Sandoval, D. C., Rodríguez-Ramos, T., Sobrino, C., Huete-Ortega, M., ... Rodríguez, J. (2013). Unimodal size scaling of phytoplankton growth and the size dependence of nutrient uptake and use. *Ecology Letters*, *16*, 371–379. https://doi.org/10.1111/ele.12052

McKie-Krisberg, Z. M., & Sanders, R. W. (2014). Phagotrophy by the picoeukaryotic green alga *Micromonas*: Implications for Arctic Oceans. *The ISME Journal*, *8*, 1953–1961. https://doi.org/10.1038/ismej.2014.16

Menden-Deuer, S., & Lessard, E. J. (2000). Carbon to volume relationships for dinoflagellates, diatoms, and other protest plankton. *Limnology and Oceanography*, *45*, 569–579. https://doi.org/10.4319/lo.2000.45.3.0569

Morán, X. A. G., López-Urrutia, Á., Calvo-Díaz, A., & Li, W. K. W. (2010). Increasing importance of small phytoplankton in a warmer ocean. *Global Change Biology*, *16*, 1137–1144. https://doi.org/10.1111/j.1365-2486.2009.01960.x

Not, F., Latasa, M., Marie, D., Cariou, T., Vaulot, D., & Simon, N. (2004). A single species, *Micromonas pusilla* (Prasinophyceae), dominates the eukaryotic picoplankton in the western English Channel. *Applied and Environment Microbiology*, *70*, 4064–4072. https://doi.org/10.1128/AEM.70.7.4064-4072.2004

Obata, H., Karatani, H., & Nakayama, E. (1993). Automated determination of iron in seawater by chelating resin concentration and chemiluminescence detection. *Analytical Chemistry*, *65*, 1524–1528. https://doi.org/10.1021/ac00059a007

Olenina, I., Hajdu, S., Edler, L., Andersson, A., Wasmund, N., Busch, S., ...Niemkiewicz, E. (2006). Biovolumes and size-classes of phytoplankton in the Baltic Sea. *HELCOM Baltic Sea Environment Proceedings* No. 106, 144 pp. ISSN: 0357-2994.

Palenik, B., Ren, Q., Dupont, C. L., Myers, G. S., Heidelberg, J. F., Badger, J. H., ... Paulsen, I. T. (2006). Genome sequence of *Synechococcus* CC9311: Insights into adaptation to a coastal environment. *Proceedings of the National Academy of Sciences of the United States of America*, *103*, 13555–13559. https://doi.org/10.1073/pnas.0602963103

Parmesan, C., & Yohe, G. (2003). A globally coherent fingerprint of climate change impacts across natural systems. *Nature*, *421*, 37–42. https://doi.org/10.1038/nature01286

Patil, V., Källqvist, T., Olsen, E., Vogt, G., & Gislrød, H. R. (2007). Fatty acid composition of 12 microalgae for possible use in aquaculture feed. *Aquaculture International*, *15*, 1–9. https://doi.org/10.1007/s10499-006-9060-3

Paulsen, M. L., Doré, H., Garczarek, L., Seuthe, L., Müller, O., Sandaa, R.-A., … Larsen, A. (2016). *Synechococcus* in the Atlantic gateway to the Arctic Ocean. *Frontiers in Marine Science*, *3*, 191. https://doi.org/10.3389/fmars.2016.00191

Raven, J. A. (1998). The twelfth Tansley Lecture. Small is beautiful: The picoplankton. *Functional Ecology*, *12*, 503–513. https://doi.org/10.1046/j.1365-2435.1998.00233.x

Reynolds, R. W., Smith, T. M., Liu, C., Chelton, D. B., Casey, K. S., & Schlax, M. G. (2007). Daily high-resolution-blended analysis for sea surface temperature. *Journal of Climate*, *20*, 5473–5496. https://doi.org/10.1175/2007JCLI1824.1.

Richardson, A. J. (2008). In hot water: Zooplankton and climate change. *ICES Journal of Marine Science*, *65*, 279–295. https://doi.org/10.1093/icesjms/fsn028

Richardson, A. J., Walne, A. W., John, A., Jonas, T. D., Lindley, J. A., Sims, D. W., … Witt, M. (2006). Using continuous plankton recorder data. *Progress in Oceanography*, *68*, 27–74. https://doi.org/10.1016/j.pocean.2005.09.011

Ruess, L., & Müller-Navarra, D. C. (2019). Essential biomolecules in food webs. *Frontiers in Ecology and Evolution*, *7*, 269. https://doi.org/10.3389/fevo.2019.00269

Sathyendranath, S., Grant, M., Brewin, R. J. W., Brockmann, C., Brotas, V., Chuprin, A., … Zibordi, G. (2018). ESA ocean colour climate change initiative (ocean_colour_cci): Version 3.1. Technical Report Centre for Environmental Data Analysis. 04 July 2018. https://doi.org/10.5285/9c334fbe6d424a708cf3c4cf0c6a53f5

Schmidt, K., Kähler, P., & von Bodungen, B. (1998). Copepod egg production rates in the Pomeranian Bay (Southern Baltic Sea) as a function of phytoplankton abundance and taxonomic composition. *Marine Ecology Progress Series*, *174*, 183–195. https://doi.org/10.3354/meps174183

Sharples, J., Moore, C. M., Hickman, A. E., Holligan, P. M., Tweddle, J. F., Palmer, M. R., & Simpson, J. H. (2009). Internal tidal mixing as a control on continental margin ecosystems. *Geophysical Research Letters*, *36*, L23603. https://doi.org/10.1029/2009GL040683

Six, C., Thomas, J.-C., Garczarek, L., Ostrowski, M., Dufresne, A., Blot, N., … Partensky, F. (2007). Diversity and evolution of phycobilisomes in marine *Synechococcus* spp.: A comparative genomics study. *Genome Biology*, *8*, R259. https://doi.org/10.1186/gb-2007-8-12-r259

Smyth, T. J., Fishwick, J. R., AL-Moosawi, L., Cummings, D. G., Harris, C., Kitidis, V., … Woodward, E. M. S. (2010). A broad spatio-temporal view of the Western English Channel observatory. *Journal of Plankton Research*, *32*(5), 585–601. https://doi.org/10.1093/plankt/fbp128

Sohm, J. A., Ahlgren, N. A., Thomson, Z. J., Williams, C., Moffett, J. W., Saito, M. A., … Rocap, G. (2016). Co-occuring *Synechococcus* ecotypes occupy four major oceanic regimes defined by temperature,

macronutrients and iron. *The ISME Journal*, *10*, 333–345. https://doi.org/10.1038/ismej.2015.115

Sutak, R., Botebol, H., Blaiseau, P.-L., Léger, T., Bouget, F.-Y., Camadro, J.-M., & Lesuisse, E. (2012). A comparative study of iron uptake mechanisms in marine microalgae: Iron binding at the cell surface is a critical step. *Plant Physiology*, *160*, 2271–2284. https://doi.org/10.1104/pp.112.204156

Tarran, G. A., & Bruun, J. T. (2015). Nanoplankton and picoplankton in the Western English Channel: Seasonality and variability from 2007–2013. *Progress in Oceanography*, *137*, 446–455. https://doi.org/10.1016/j.pocean.2015.04.024

Taylor, A. H., Allen, J. I., & Clark, P. A. (2002). Extraction of a weak climate signal by an ecosystem. *Nature*, *416*, 629–632. https://doi.org/10.1038/416629a

Ting, C. S., Rocap, G., King, J., & Chisholm, S. W. (2002). Cyanobacterial photosynthesis in the ocean: The origins and significance of divergent light-harvesting strategies. *Trends in Microbiology*, *10*, 134–142. https://doi.org/10.1016/s0966-842x(02)02319-3

Tsai, A.-Y., Chiang, K.-P., Chan, Y.-F., Lin, Y.-C., & Chang, J. (2007). Pigmented nanoflagellates in the coastal western subtropical Pacific are important grazers on *Synechococcus* populations. *Journal of Plankton Research*, *29*, 71–77. https://doi.org/10.1093/plankt/fbl058

Watson, R. A., Green, B. S., Tracey, S. R., Farmery, A., & Pitcher, T. J. (2016). Provenance of global seafood. *Fish and Fisheries*, *17*, 585–595. https://doi.org/10.1111/faf.12129

Wilhelm, S. W., & Trick, C. G. (1994). Iron-limited growth of cyanobacteria: Multiple siderophore production is a common response. *Limnology and Oceanography*, *39*, 1979–1984. https://doi.org/10.4319/lo.1994.39.8.1979

Woodward, E. M. S., & Rees, A. P. (2001). Nutrient distributions in an anticyclonic eddy in the North East Atlantic Ocean, with reference to nanomolar ammonium concentrations. *Deep Sea Research Part II: Topical Studies in Oceanography*, *48*, 775–794. https://doi.org/10.1016/S0967-0645(00)00097-7

Yool, A., Popova, E. E., & Coward, A. C. (2016). Future change in ocean productivity: Is the Arctic the new Atlantic? *Journal of Geophysical Research: Oceans*, *120*, 7771–7790. https://doi.org/10.1002/2015JC011167

SUPPORTING INFORMATION

Additional supporting information may be found online in the Supporting Information section.